HOP, J., STØRE, A., FOOSNÆS, T., AND ØYE, H.A. Chemical and physical changes of cathode carbon by alumimium electrolysis. *VII International Conference on Molten Slags Fluxes and Salts,* The South African Institute of Mining and Metallurgy, 2004.

Chemical and physical changes of cathode carbon by aluminium electrolysis

J. HOP*, A. STØRE†, T. FOOSNÆS‡, and H.A. ØYE‡
**Hydro Aluminium a.s. T&OS, Øvre Ardal, Norway*
†SINTEF Materials Technology, Trondheim, Norway
‡Department of Materials Technology, Norwegian University of Science and Technology, Norway

The carbon cathode for aluminium electrolysis is also part of the container of the process. In order to understand the behaviour and possible failure of the cathode, detailed material properties under operating conditions are needed. The paper reports experimental studies of bath and sodium infiltration, graphitization with time, loss of strength due to sodium, sodium expansion as function of pressure, as well as creep due to the developed stresses. As an example, sodium and thermal expansion data are used to calculate strain-stress models of realistic cell designs, and possible design weakness can be pointed out.

Keywords: carbon, cathodes, sodium expansion, strength, graphitization, creep

Introduction

Aluminium is produced in electrolysis cells:

$$Al_2O_3\left(\text{dissolved in } Na_3AlF_6, AlF_3, CaF_2\right)+1.5C(\text{anode}) \xrightarrow{960^\circ C} 2Al(1)+1.5CO_2(g) \quad [1]$$

The process is carried out in a tray whose base is lined with carbon blocks and carbon ramming paste (Figure 1). The sides are either carbon or silicon nitride-bonded SiC blocks. No materials can, however, withstand the combined action of liquid aluminium and the CO_2 saturated fluoride melt. The heat balance of cells is adjusted to produce a protective ledge at the sides. The temperature of the cathode will normally be about 960°C on the top and 910°C at the bottom, i.e., only slightly below the liquidus temperature of the electrolyte.

The most common cathode block materials are[1]

- *GCA*—gas or kiln calcined anthracite, with 30–50% graphite filler, blocks baked to 1000–1200°C. Porosity 16–19%.
- *ECA*—electrocalcined anthracite, partly graphitized, with 30% graphite filler, blocks baked to 1000–1200°C. Porosity 16–20%.
- *SG*—Semigraphitic, all aggregates graphitized, baked to 1000–1200°C. Porosity 19–23%.
- *SGZ*—semigraphitized, graphitizable filler, whole blocks calcined above 2300°C. Porosity 23–26%.
- *GZ*—graphitized, baked at 2800°C.

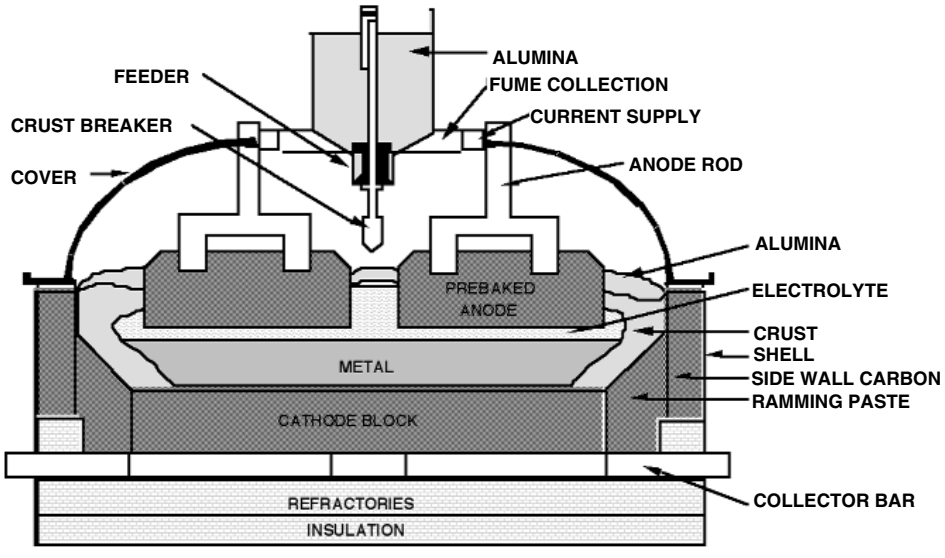

Figure 1. Diagram of a prebaked cell

Cell life

An aluminium reduction cell has to be stopped when the electrolyte or liquid aluminium is about to penetrate the steel shell. Early failure may be caused by materials, design, start-up and operation, but materials are increasingly important as steadily longer life is wanted. Earlier, 1 200 days were considered satisfactory, today a minimum of 2 000 days is expected and the aim is to obtain 3 000–4 000 days' life. A detailed knowledge of the materials properties of the cathode materials is an important tool to understand the behaviour during the cell's life. In addition to chemical changes within the materials, the present paper addresses mechanical properties. The mechanical properties change with time, especially within the cathode. Different materials have been studied, and finally stress-strain models are presented based on earlier laboratory studies.

Chemical reaction and graphitization

The electrolyte wets carbon poorly, and in order to obtain a smooth electrolysis, a liquid pool of aluminium, 15–30 cm, is kept at the bottom. Nevertheless, a thin layer of electrolyte stays between the aluminium and carbon, manifested by the absorption of the electrolyte in the carbon, resulting in a density increase of up to 50 wt%. The mechanism is initial absorption of sodium in micropores followed by the penetration of electrolyte into the pores as well as changes in the carbon structure. The penetration will only stop when the electrolyte and its reaction products reach the solidus temperatures in the refractory. A large number of industrial cathodes was analysed for salt content, and Figure 2 gives the average concentration of the different compounds as a function of time[2]. The chemical reactions occurring in the carbon cathode can be understood from thermodynamics (Table I).

Graphitization usually needs very high temperatures and full graphitization of petroleum coke is only obtained at temperatures above 3000°C. However, anthracitic materials graphitize at electrolysis temperatures manifested by change of electrical and thermal conductivity with time (Figure 3)[4].

Loss of strength

For some materials, sodium absorption leads to loss of strength due to microcracking. Figure 4a shows the equipment for the bending strength measurements during electrolysis. Bending tests are performed *in situ*. Anthracitic materials lose more than half the strength but regain some (Figure 4b). The semi-graphitized material (Figure 4e) is unaffected, while the semi-graphitic materials become intermediate between the semi-graphitized and anthracitic materials (Figure 4c,d). The present laboratory study is carried out at CR = 4.0, but the effects are much smaller in industrial electrolysis with CR = 2.3.

Sodium expansion

Sodium expansion studies are carried out in the equipment shown in Figure 5. Figure 6 gives the sodium expansion for

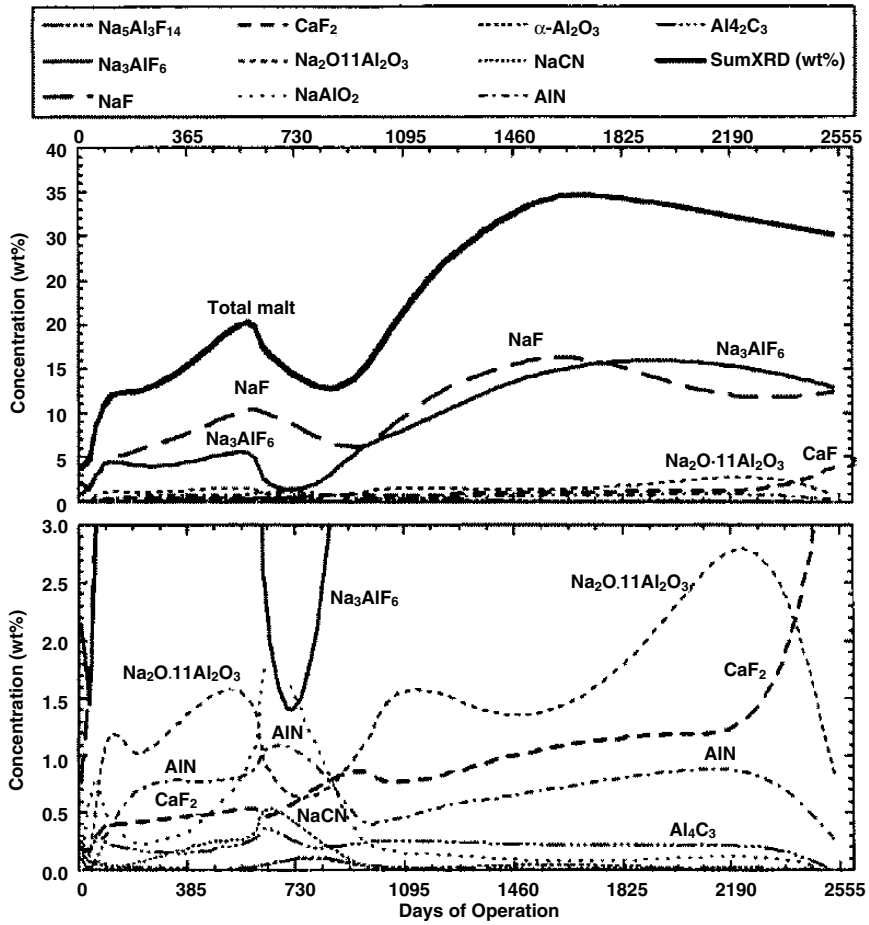

Figure 2. Evolution of the melt component phases (wt%) with time given as the average in the lining[2]

Table I
Chemical reactions grouped in classes, with the Gibbs free energy of reaction, ΔG^o, at 950°C (1223 K) calculated using SOLGAS/ChemSage[3]*)

		ΔG^o(kJ)
	The origin of Na(C), CO, NaCN and Na_2CO_3	
1	6 NaF + Al(l) = Na_3AlF_6(l) + 3 Na(C)	+41.7
2	0.5 O_2(g) + C(s) = CO(g)	-220.0
3	4.5 CO(g) + 3 Na(C) = 1.5 Na_2CO_3(l) + 3 C(s)	-209.1
4	1.5 N_2(g) + 3 Na(C) + 3 C(s) = 3 NaCN(l)	-164.7
	The reactions that change the cryolite ratio)**	
5	0.75 Na_3AlF_6(l) + 1.5 CO(g) + 3 Na(C) = 0.75 $NaAlO_2$ (s) + 4.5 NaF(l) + 1.5 C(s)	-346.5
6	0.75 Na_3AlF_6(l) +1.5 Na_2CO_3(l) +1.5 C(s) = 3 CO(g) + 0.75 $NaAlO_2$(s) + 4.5 NaF(l)	-137.8
7	Na_3AlF_6(l) + 0.5 N_2(g) + 3 Na(C) = AlN(s) + 6 NaF(l)	-225.0
8	1.5 Na_3AlF_6 (l) + 1.5 NaCN(l) + 3 Na(C) = 1.5 AlN(s) + 9NaF(l) + 1.5 C(s)	-255.0
	The reactions that consume NaCN are Equation 8 and	
9	3 Al_2O_3(s) + 1.5 NaCN(l) + 3 Na(C) = 4.5 $NaAlO_2$(s) + 1.5 AlN(s) + 1.5 C(s)	-214.8
	Additional formation of NaAlO2	
10	3 AlN(s) + 6 CO(g) + 3 Na(C) = 3 $NaAlO_2$(s) + 6 C(s) + 15 N_2(g)	-711.0
11	Al_2O_3(s) + CO(g) + 2 Na(C) = 2 $NaAlO_2$(s) + C(s)	-217.7
	Formation of Al_4C_3	
12	Na_3AlF_6(l) + 3 Na(C) + 0.75 C(s) = 0.25 Al_4C_3(s) + 6 NaF(l)	-74.3
13	2 Al_2O_3(s) + 0.75 C(s) + 3 Na(C) = 3 $NaAlO_2$ (s) + 0.25 Al_4C3 (s)	-47.5

*) In Equations [9], [11] and [13] the alumina data are for α-Al_2O_3 as data for the actual similar compound β-Al_2O_3 ($Na_2O{\cdot}11Al_2O_3$) was not found. In Equations with Na(C) data for Na(l) were used. The chosen standard state for sodium means that the real ΔG is somewhat more negative when Na(C) is present on the right side of the equation and somewhat more positive when Na(C) is present on the left side.

**) CR = Mole NaF/Mole AlF_3

Thermal conductivity of used cathode bottom blocks of type A2 as function of temperature

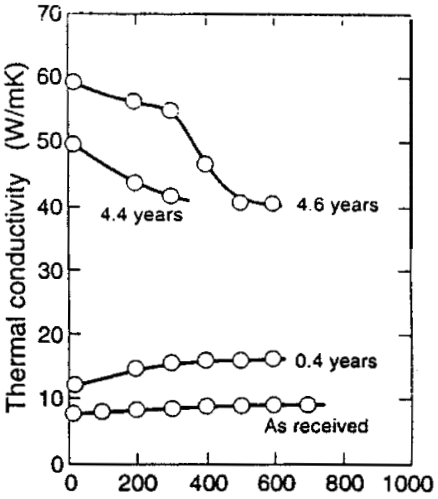

Electrical resistivity of used cathode bottom blocks of type A2 for the temperature range up to 1000°C

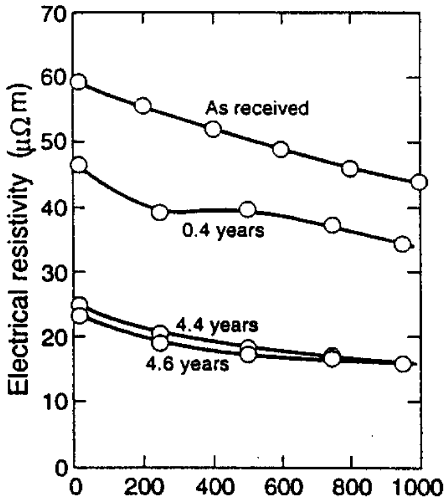

Thermal conductivity of used cathode bottom blocks of type B3 as function of temperature

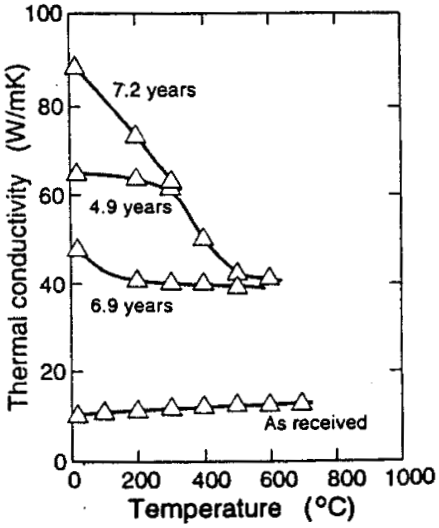

Electrical resistivity of used cathode bottom blocks of type B3 for the temperature range up to 1000°C

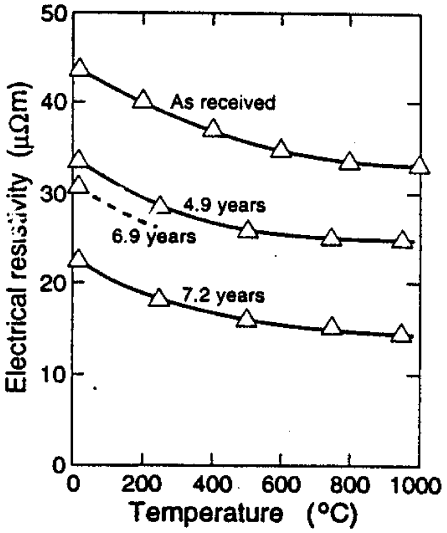

Figure 3. Electrical and thermal conductivity as a function of temperature and time for two anthracitic materials[4]

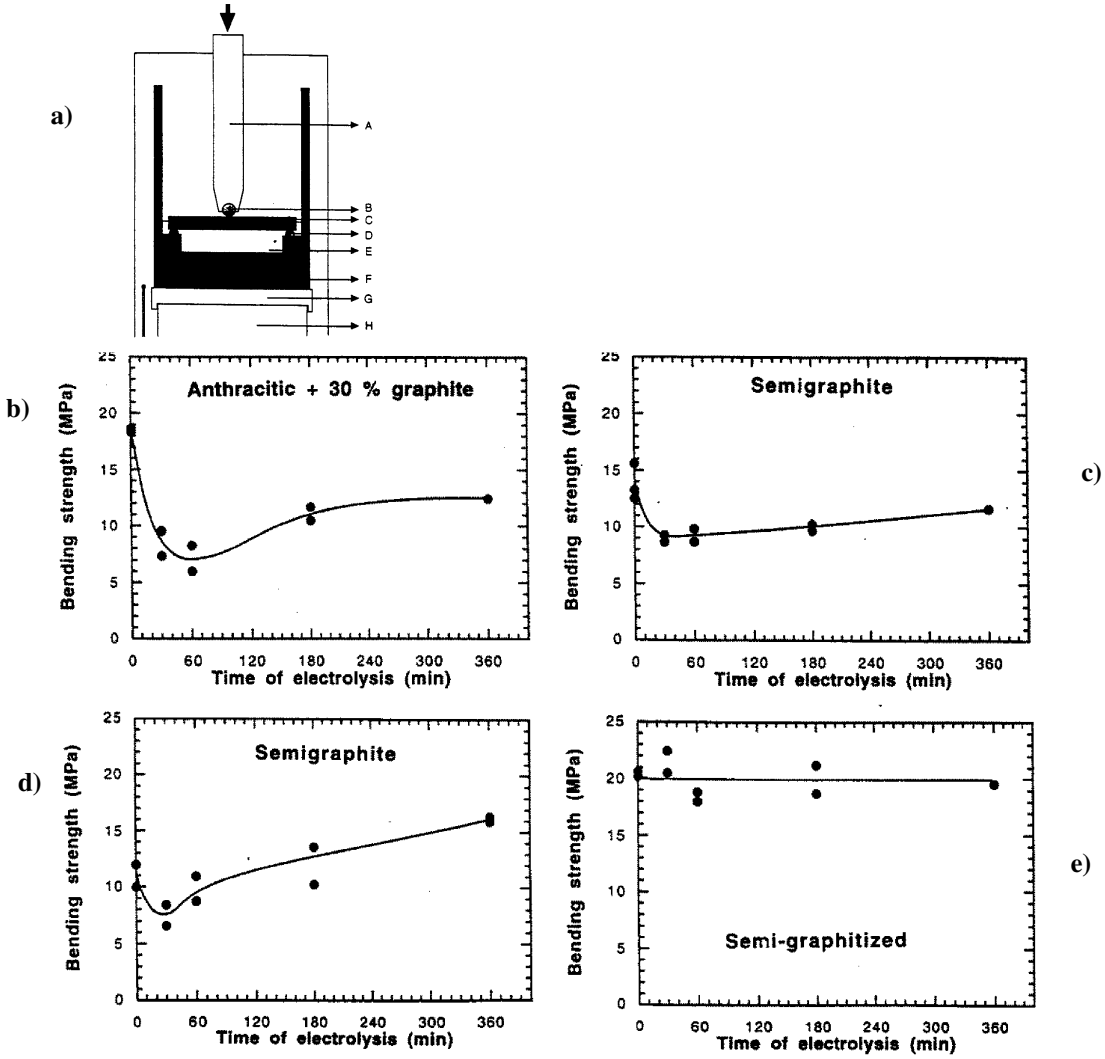

Figure 4. Bending strength under electrolysis conditions. CR = 4.0. Temperature 980°C. The electrolyte is underneath the carbon sample. a) Equipment—A: piston, B: load bar, C: cathode sample, D: alumina support, E. cryolite melt, F: graphite crucible. G: support, H: current extension. b) – d) Bending strength as function of electrolysis time

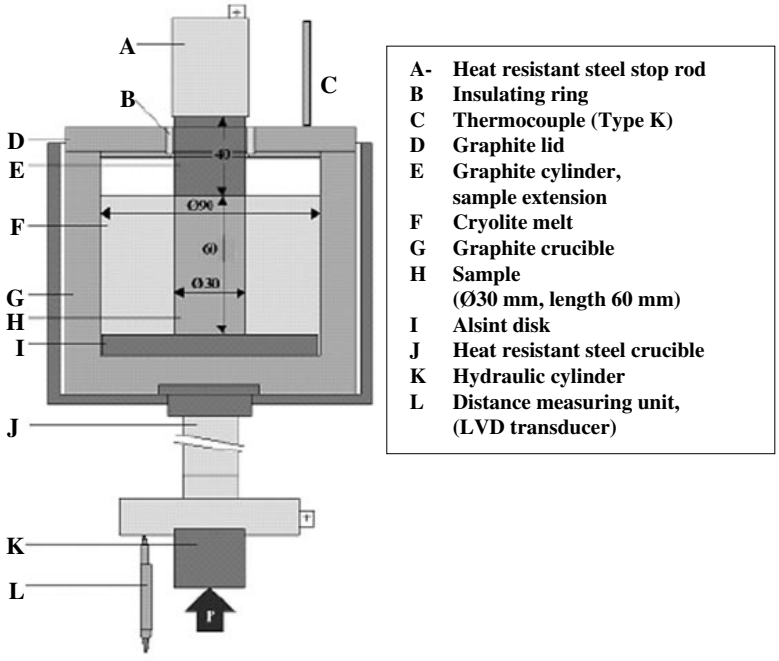

Figure 5. Apparatus to measure sodium expansion[5]

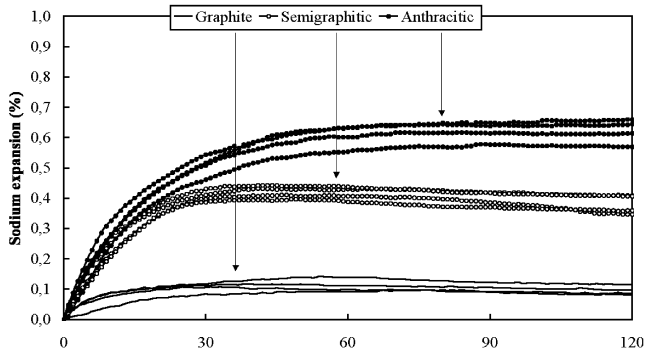

Figure 6. Sodium expansion for 3 different commercial materials. Pressure 5 Mpa

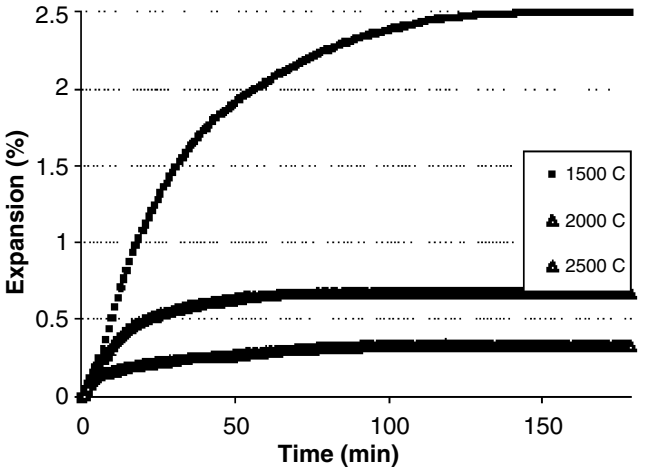

Figure 7. Sodium expansion at a pressure of 2.3 MPa laboratory produced materials with petroleum coke heat treated to different tempera-tures

3 materials, graphitic, semi-graphitic and anthracitic. Figure 7 shows sodium expansion in laboratory-made materials where petroleum coke with different heat treatment temperatures is used. The expansion decreases with increasing heat-treatment temperature (i.e. increased graphitization). The expansion for petroleum coke heat-treated to 1500°C is so high that the material is unacceptable as a cathode material. For low heat-treatment temperature, anthracite is better. The sodium expansion also increases with increased CR (mole NaF/mole AlF_3) and increased current density. The higher expansion at higher CR is a direct consequence of the equilibrium given as Equation [1] in Table I. Similarly, the increase with current density is an indirect consequence of Equation [1]. As sodium is the current carrier to the cathode while aluminium is discharged, an enhancement of NaF is expected on the cathode surface. Figure 8 shows sodium expansion as function of pressure[6]. The expansion is measured relative to a pressurized sample 5MPa reduces the expansion with 50%.

Creep

The cathode materials are subject to pressure due to thermal and sodium expansion against a strong steel shell. These pressures will not only lead to elastic contractions (E-modulus) but also to creep of the carbon blocks. Creep was studied in the equipment on Figure 9.

This equipment eliminates creep of the apparatus. Figure 10 shows creep and creep recovery for different pressures. The creep is much higher during electrolysis conditions, which again can be attributed to the action of sodium (Figure 11).

Figure 12 shows some creep experiments for an extended time period. The creep is very fast in the beginning, but then a hardening effect sets in. The mechanism of the creep is not related to the creep observed for graphite at 3000°C, but crack development similar to what is observed for concrete.

Discussion and application

The object of the present studies is to obtain more realistic thermal-electrical-mechanical models of aluminium cells during electrolysis. A realistic thermoelectrical model must take into consideration that the electrical and thermal

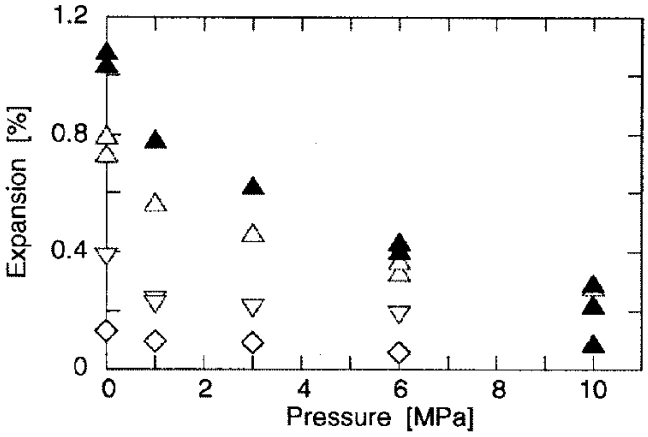

Figure 8. Expansion of carbon cathode samples due to sodium penetration. Temperature 980 ± 10°C. CR = 4. CD = 0.65 A/cm². Open triangle: ECA II. Filled triangle ECA ⊥. Open upside-down triangle: SGZ II. Open diamond: GZ II (II Parallel to extrusion,⊥ perpendicular to extrusion)

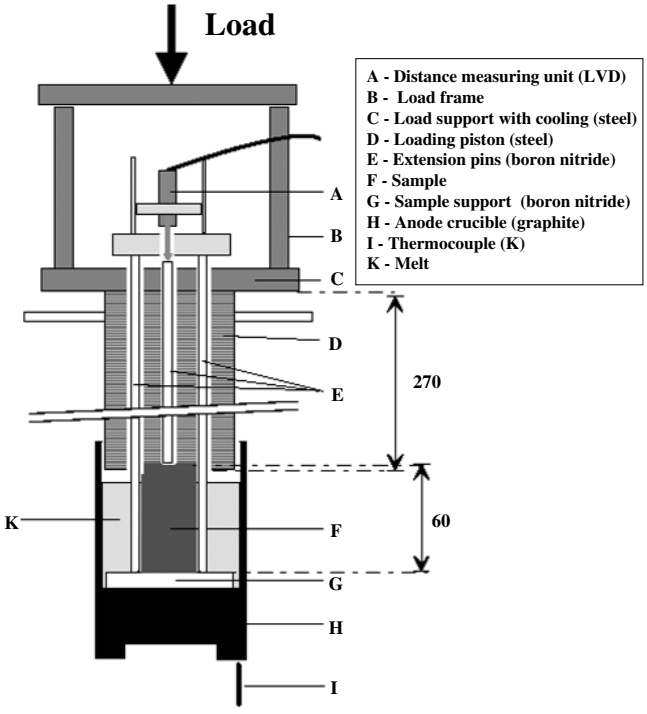

Figure 9. Cross-section of apparatus for creep measurements

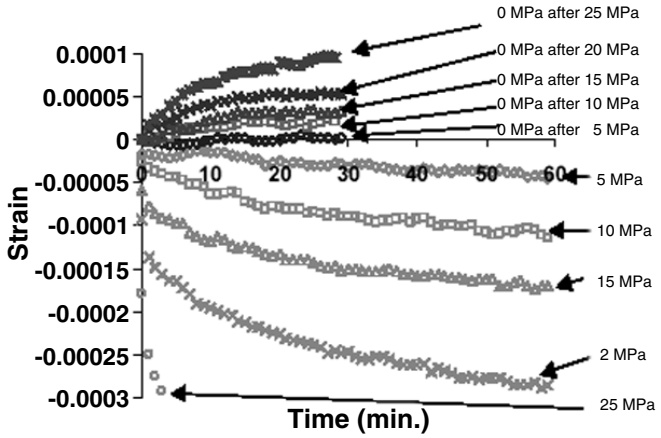

Figure 10. Creep and recovery of an anthracitic material at 5 pressure levels

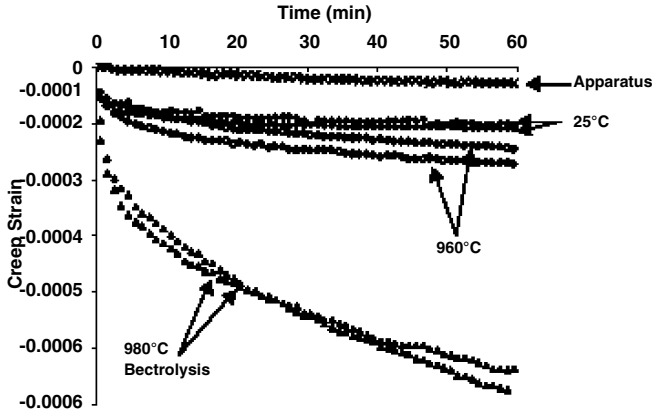

Figure 11. Creep strain of two parallels for an anthracitic material with a pressure of 15 MPa. The near negligible creep of the apparatus is shown as the upper curve

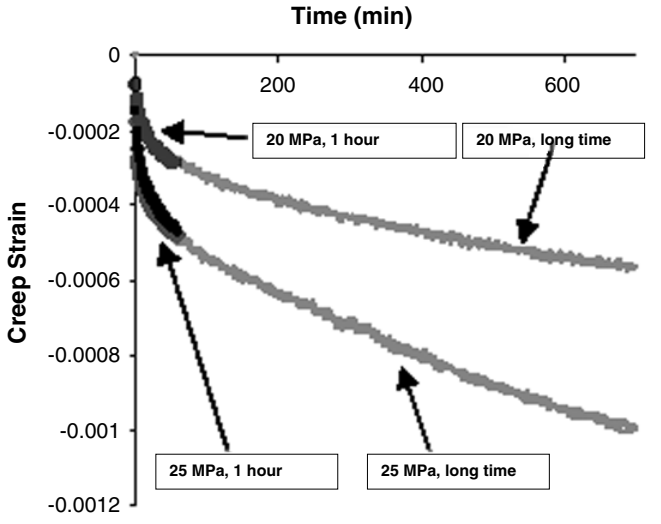

Figure 12. Creep at two pressure levels for an extended period

conductivities change with temperature and time. The studies also show that the room temperature strength of anthracitic materials may be misleading as the material may lose half its strength due to the action of sodium. A strain-strength model should also take creep into consideration.

The data also give a useful base for strain-stress modelling as guidance for improving the cell design. The models are especially valuable to pinpoint areas with high stress gradients where cracking may occur. The following measured or known properties are introduced: thermal conductivity, specific heat, density, thermal expansion, Young's modulus, Sodium expansion as a function of concentration and pressure, and Sodium diffusion coefficients. Using given geometric sizes for the different materials, the model can give concentration and strain-stress calculated as function of time. Figure 13 shows such a model[7]. In this prototype the strain of the steel sidewall had been measured. As the main cause of expansion is due to sodium, the sodium diffusion coefficient could be used to calibrate the model. Due to the crushable vermiculite (Material 9 in Figure 13), the X-direction stress is even after 400 days of operation (Figure 14). This is contrary to

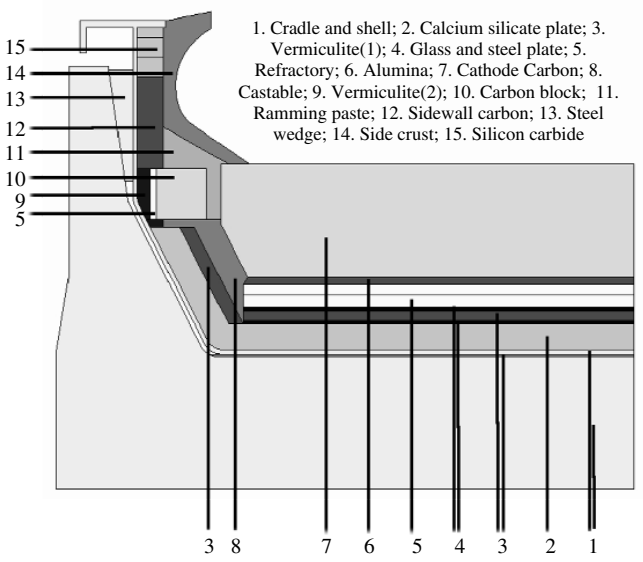

Figure 13. Structure and materials of the prototype reduction cell (transverse section)

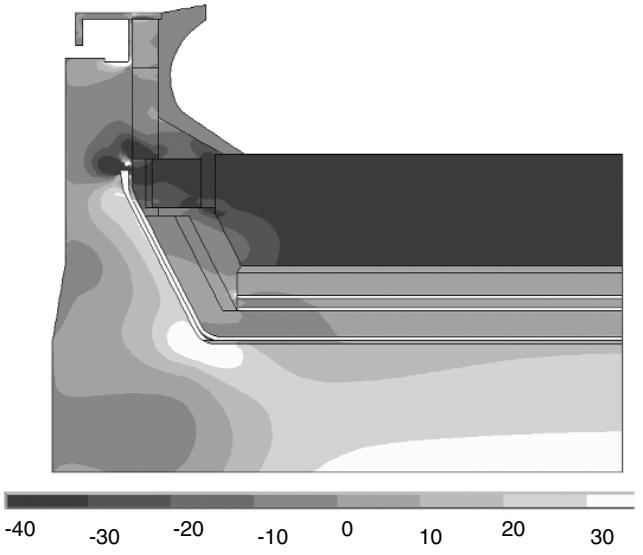

Figure 14. X-direction stress after 400 days in MPa

another model when the crushable material is only in the lower part of the cathode and a strong X-direction stress gradient develops in the middle of the cathode. This other construction is, hence, vulnerable to horizontal lamination, which was also found in practice. In future models creep will also be included as stresses calculated are too high.

References

1. SØRLIE, M. and ØYE, H.A. *Cathodes in Aluminium Electrolysis*. 2nd edition. Aluminium-Verlag, Düsseldorf (1994) 408 pp.
2. LOSSIUS, L.P. and ØYE, H.A. Melt Penetration and Chemical Reactions in Cathodes during Aluminium Electroysis. II. *Industrial Cathodes. Met. Mat. Trans.* 31 B (2000) pp. 1213–1224.
3. *ChemSage Application Software for Thermodynamical Calculations with SGTE Pure Substance Databases SOR94G02 (organic) and SPS94T02 (Inorganic) ChemSage Handbook*, Version 3.0.1, GTT Technologies, Herzogenrath, 1994.
4. SØRLIE, M., GRAN, H., and ØYE, H.A. Property Changes of Cathode Lining Materials during Cell Operation. *Light Metals* 1995, pp. 497–506.
5. SCHREINER, H. and ØYE, H.A. Sodium Expansion of Cathode Materials under Pressure. *Light Metals* 1995, pp. 463–472.
6. ISO/FD 15379-1: 2003 (E). Carbonaceous materials for the production of aluminium–Cathode is block materials–Part 1: Determination of the expansion due to sodium penetration with application of pressure.
7. SUN, Y., WANG, Q., RYE, K.Å., SØRLIE, M., and ØYE, H.A. Modelling of Thermal and Sodium Expansion in Prebaked Aluminium Reduction Cells. *Light Metals* 2003, pp. 605–610.